# Fischer-Tropsch synthesis on the cobalt impregnated catalyst using carbon-coated Ni/SiO$_2$

**Hyun-Mo Koo, Gui Young Han, and Jong Wook Bae[†]**

School of Chemical Engineering, Sungkyunkwan University (SKKU), Suwon, Gyeonggi-do 16419, Korea
(*Received 15 June 2015 • accepted 4 December 2015*)

**Abstract**−Carbon-coated Ni/SiO$_2$ prepared by dry reforming of CH$_4$ with CO$_2$ was applied for the preparation of the cobalt-based Fischer-Tropsch synthesis (FTS) catalyst with 20 wt%Co to elucidate the metal-support interaction to FTS activity after carbon depositions on the Ni/SiO$_2$. The deposited carbons on the reforming catalyst of Ni/SiO$_2$, which were mainly in the form of filamentous or encapsulated carbons, largely increased CO conversion compared with the fresh Ni/SiO$_2$ without a significant variation of hydrocarbon distributions. The deposited carbons on the Ni/SiO$_2$ play an important role in increasing the reducibility of cobalt oxides due to a mitigated metal-support interaction. The enhanced catalytic activity during FTS reaction is mainly attributed to the proper modification of the Ni/SiO$_2$ surfaces with encapsulated carbons on the exposed nickel surfaces, which largely alters the reducibility of cobalt oxides by reducing the interaction of cobalt particles with the carbon-coated Ni/SiO$_2$ surfaces.

Keywords: Fischer-Tropsch Synthesis (FTS), Cobalt, Ni/SiO$_2$, Carbon Deposition from Dry Reforming, Metal-support Interaction

## INTRODUCTION

Considerable research has been carried out to improve the catalytic performance of Fischer-Tropsch synthesis (FTS) reaction and to optimize the fully-integrated Gas-To-Liquids GTL process, which can produce clean fuels from alternative feedstock such as natural gas or shale gas and coal [1]. Various active metals such as Ru, Fe, Co, and Ni can be used for FTS reaction through CO hydrogenation reaction with different activities and product distributions according to the types of active metals. Since the proper selection of irreducible metal oxide supports such as silica, alumina, titania and carbon can alter the reduction degrees and the particle sizes of cobalt species with different metal-support interactions, the FTS activity and product distribution can be significantly altered [1-8]. Among them, cobalt-supported on the Al$_2$O$_3$ catalyst has been known to be more active with a higher resistance to deactivation and a lower water gas shift activity by producing linear heavy hydrocarbons during a low temperature FTS reaction [1,6]. However, some commercially available irreducible metal oxides such as alumina, silica, and titania have been also reported to form inactive cobalt phases such as spinel structural cobalt aluminates (CoAl$_2$O$_4$), cobalt silicate (CoSiO$_2$) or CoTiO$_4$ during a calcination step and/or FTS reaction. These inactive phases can form strong metal-support interactions with cobalt particles, and can significantly reduce the FTS activity and accelerate catalyst deactivation [1,2-4,6,8]. Since the low degree of reduction of cobalt particles through a formation of strong metal-support interaction can be responsible for decreasing the number of the exposed active metal atoms, some novel metals such as Ru, Pt and Re can be used to enhance the reducibil-

ity of the cobalt oxides [3]. Therefore, carbon supports have been largely investigated to suppress the formation of inactive cobalt phases by reducing metal-support interactions [3-5]. For example, the metal-support interaction on Co/CNT can be weakened, and it has resulted in significantly improving the reducibility of the supported cobalt particles [4]. Novel carbon materials such as carbon nanotube, carbon nanofiber and regular mesoporous carbon can provide new opportunities for preparing superior FTS catalysts due to their weak interaction with supported metals [2-4].

To verify the effects of coke deposition on the used Ni/SiO$_2$ to the FTS activity, a simple and recyclable carbon deposited Ni/SiO$_2$ support was prepared by dry CO$_2$ reforming with CH$_4$ (CDR) with an insignificant coke deposition in a fluidized-bed reactor through the following reaction to produce syngas with a H$_2$/CO molar ratio of around 1.0 [9,10].

$$CH_4 + CO_2 = 2CO + 2H_2 \qquad \Delta H = 247.3 \text{ kJ/mol}$$
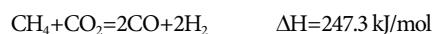
In the present investigation, carbon-coated Ni/SiO$_2$, having a coke content of ~3 wt% [10] in the form of the encapsulated carbons from our previous work, was further applied to prepare the cobalt-based FTS catalyst. The activity was compared with the fresh Ni/SiO$_2$ support to verify the roles of the carbon encapsulation of the Ni/SiO$_2$ during CDR reaction in terms of metal-support interaction. The different catalytic activities are mainly attributed to the mitigated metal-support interaction due to the carbon decoration on the Ni/SiO$_2$ support.

## EXPERIMENTAL

### 1. Preparation of Co/Carbon-coated Ni/SiO$_2$ Catalyst and Activity Evaluation

The supported cobalt-based FTS catalyst was prepared by wet impregnation method using the support of Ni/SiO$_2$ before and after

[†]To whom correspondence should be addressed.
E-mail: finejw@skku.edu

**Table 1. Physicochemical properties of the CNS catalysts**

| Notation | N$_2$ sorption | | | XRD[a] | | H$_2$ Chemisorption | TPR | TGA[b] |
|---|---|---|---|---|---|---|---|---|
| | Surface area (m$^2$/g) | Pore volume (cm$^3$/g) | Average pore diameter (nm) | Co$_3$O$_4$ particle size (nm) | Co particle size (nm) | Surface area of Co (m$^2$/g$_{Co}$) | (P(I)+P(II)) /total | Coke (wt%) |
| CNS | 188 | 0.33 | 7.1 | 14.9 | 11.2 | 37.6 | 0.298 | 0 |
| CNS(C) | 194 | 0.36 | 7.3 | 15.8 | 11.8 | 34.3 | 0.400 | 3.2 |

[a]The particle size of the Co$_3$O$_4$ was calculated using the FWHM value at the most intense characteristic diffraction peak of $2\theta=44.7°$ on the fresh CNS catalysts; and the size of metallic cobalt was also calculated from the Co$_3$O$_4$ particle sizes by using the correlation for a relative molar volume of metallic cobalt species with the equation of d(Co$^0$)=0.75×d(Co$_3$O$_4$)

[b]The deposited amount of coke precursors was represented by wt% of the coke (from TGA) based on the total weight of 15 wt%Ni/SiO$_2$ after CDR reaction reacted at a molar ratio of CH$_4$/CO$_2$=2 in a fluidized-bed reactor

the CDR reaction. The CDR reaction was previously carried out in a fluidized-bed reactor using 100 g of 15 wt%Ni/SiO$_2$ catalyst, which was prepared by incipient wetness impregnation using SiO$_2$ support having a surface area of 250 m$^2$/g and nickel nitrate precursor in aqueous solution. After the CDR reaction at somewhat severe reaction conditions for the preferential coke formation such as P= 0.1 MPa, T=650 $^o$C and CH$_4$/CO$_2$=2 for 4 h, the carbon-coated 15 wt%Ni/SiO$_2$ was obtained with a total deposited coke amount of 3.2 wt%, verified by thermal gravimetric analysis as shown in Table 1. As shown in Fig. S1, conversions of CH$_4$ and CO$_2$ in a fluidized bed reactor at a CH$_4$/CO$_2$ feed molar ratio of 2 and a total gas velocity of 2 U$_{mf}$, where it stands for a minimum fluidization velocity with a linear velocity of 2.16 cm/s on the Ni/SiO$_2$ catalyst, were found to be around 45 and 55%, respectively, with more or less coke deposition. For comparison, regular mesoporous carbon support of CMK-3 was also used as a supporting material. Using the fresh and carbon-coated used Ni/SiO$_2$ and CMK-3 support, the cobalt precursor of Co(NO$_3$)$_2$·6H$_2$O was subsequently impregnated on the supports at a fixed 20 wt%Co using excess deionized water in a rotary evaporator at ambient temperature for 3 h, and excess water was evacuated at 50 $^o$C under vacuum condition. The as-prepared samples were further dried at 110 $^o$C for 12 h, followed by calcining at 400 $^o$C for 3 h under air atmosphere. The as-prepared catalysts are denoted as CNS (by using fresh Ni/SiO$_2$ before CDR reaction) and CNS(C) (by using carbon-coated Ni/SiO$_2$ after CDR reaction) and Co/CMK-3 (by using CMK-3 without calcination), where C, N, S and (C) represents cobalt, nickel, SiO$_2$, and carbon deposition after CDR reaction, respectively.

The catalytic activity was evaluated in a fixed-bed tubular reactor (outer diameter of 9.5 mm) with a catalyst loading of 0.2 g. Before the FTS reaction, the CNS catalysts were activated under the flow of reduction gas containing 5 vol%H$_2$ balanced with N$_2$ at 400 $^o$C for 12 h. After the reduction, the mixed reactants of syngas (H$_2$/CO molar ratio of 2) with N$_2$ as an internal standard gas were fed into the tubular reactor, with a composition of 31.5%CO, 63.0%H$_2$ and 5.5%N$_2$. The FTS reaction lasted about 20 h at the following reaction conditions: P=2.0 MPa, T=230 $^o$C and WHSV (weight hourly space velocity)=4,000 L (mixed gas)/(kg$_{cat}$·h) using the FTS catalyst having a particle size of 50-120 μm. The effluent gases from the reactor after passing through wax trap kept at 60 $^o$C were analyzed by on-line gas chromatograph (Younglin GC, YL6100) with thermal conductivity detector (TCD) connected with GS-GASPRO

capillary column to analyze N$_2$, CO, H$_2$, CH$_4$, CO$_2$. Flame-ionized detector (FID) connected with Carboxen 1000 packed column was also applied to analyze the hydrocarbons formed during FTS reaction. CO conversion was calculated by correcting the intensity changes of internal standard gas of N$_2$ using an equation of [(CO$_{inlet}$− CO$_{outlet}$)/CO$_{inlet}$]*100, and product distributions were also calculated based on the total carbon-balances.

**2. Catalyst Characterizations**

BET surface area, pore volume and average pore diameter of the fresh CNS catalysts before FTS reaction were characterized from N$_2$ adsorption-desorption isotherm obtained at −196 $^o$C by using a constant volume adsorption instrument, Micromeritics ASAP-2020. The pore size distribution of the catalysts was also plotted by using BJH (Barrett-Joyner-Halenda) method from the N$_2$ desorption isotherm branch.

The surface area of metallic cobalt on the FTS catalysts was determined by H$_2$-chemisorption on Micromeritics ASAP-2020C equipment. Prior to H$_2$ chemisorption, the as-prepared fresh catalysts were previously reduced under a flow of H$_2$ at 400 $^o$C for 12 h with a heating rate of 10 $^o$C/min, which was the same condition with a reduction condition before the FTS reaction. After reduction, two consecutive H$_2$ adsorption isotherms were measured at 100 $^o$C for measuring the chemisorbed H$_2$ by subtracting the physisorbed amount of H$_2$ with a stoichiometry of H/Co=1. The degree of reduction of Co$_3$O$_4$ on the CNS was also measured by O$_2$ titration method, and it was calculated by using the equation of [amount of O$_2$ consumed during O$_2$ titration]/[theoretical amount of O$_2$ consumption after a full reduction of Co$_3$O$_4$ with the assumption of (3Co+2O$_2$→Co$_3$O$_4$)]×100.

Wide-angle powder X-ray diffraction (XRD) analysis of the fresh and used CNS catalysts was characterized by D8 ADVANCE using a Cu-K$_\alpha$ radiation (0.15406 nm) operating at 40 kV and 100 mA in the range of 5-80$^o$ at a scanning rate of 5$^o$/min. The average particle size of the Co$_3$O$_4$ on the fresh and used CNS catalysts was calculated by Scherrer equation. The value of full width at half maximum (FWHM) at the most intensive characteristic peak of $2\theta=$ 44.7$^o$ was used to estimate the Co$_3$O$_4$ particle sizes on the fresh CNS catalysts. In addition, the particle size of metallic cobalt was also estimated by using the correlation of the relative molar volume of metallic cobalt with Co$_3$O$_4$ such as d(Co$^0$)=0.75×d(Co$_3$O$_4$) [11].

Temperature programmed reduction (H$_2$-TPR) patterns of the fresh CNS catalysts were analyzed to determine the reduction be-

haviors of the cobalt oxides and nickel oxides by using BELCAT-M instrument supplied by BEL JAPAN INC. Before TPR experiment, the sample with 30 mg was pretreated under Ar flow at 250 °C for 1 h to remove the adsorbed water followed by cooling to 50 °C. Then, the reduction gas containing 10 vol%$H_2$ balanced with Ar was fed over the sample by increasing temperature to 900 °C with the ramping rate of 20 °C/min. The effluent gas was passed over a molecular sieve trap to remove water formed during TPR experiment, and the effluent gases were analyzed by using TCD.

The surface morphologies and particle size distribution of the cobalt species on the fresh and used CNS catalysts were characterized by scanning electron microscopy (SEM) with JEOL instrument (JSM6700F) and transmission electron microscopy (TEM) of Tecnai G2-20 instrument operating at 200 kV, respectively.

Thermal gravimetric analysis (TGA) of the used reforming catalyst of Ni/SiO₂ (after CDR reaction for 4 h in a fluidized-bed reactor with 100 g catalyst) was carried out using TA instrument. For TGA analysis, 30 mg of the used Ni/SiO₂ was heated from 30 to 900 °C with a ramping rate of 10 °C/min under air environment with a flow rate of 30 ml/min. The variation of weight loss of the used Ni/SiO₂ was recorded through TGA.

## RESULTS AND DISCUSSION

### 1. Physicochemical Properties of the CNS Catalysts

The surface area, pore volume and average pore diameter of the fresh CNS catalysts are summarized in Table 1. The surface area was found to be 188 and 194 m²/g on the CNS and CNS(C), respectively. It was slightly reduced from 250 m²/g of the fresh Ni/SiO₂ due to the coke deposition on the surfaces after CDR reaction and the subsequent cobalt deposition on the CNS catalysts. The pore volume and average pore size showed similar trends with the values of 0.33-0.36 cm³/g and 7.1-7.3 nm, respectively. From the N₂ adsorption-desorption isotherms as shown in Fig. S2, the fresh CNS catalysts showed a typical type-IV isotherm, which mainly originated from the characteristics of SiO₂ support. As shown in Fig. 1, the pore size distribution on the fresh CNS catalysts showed three different pore diameters, with the largest peak intensity at a
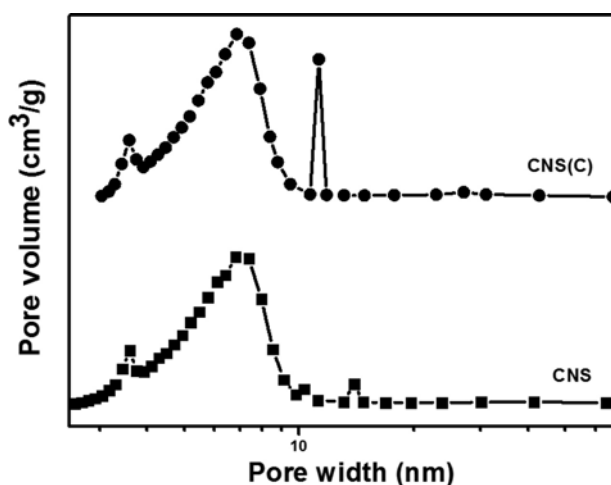


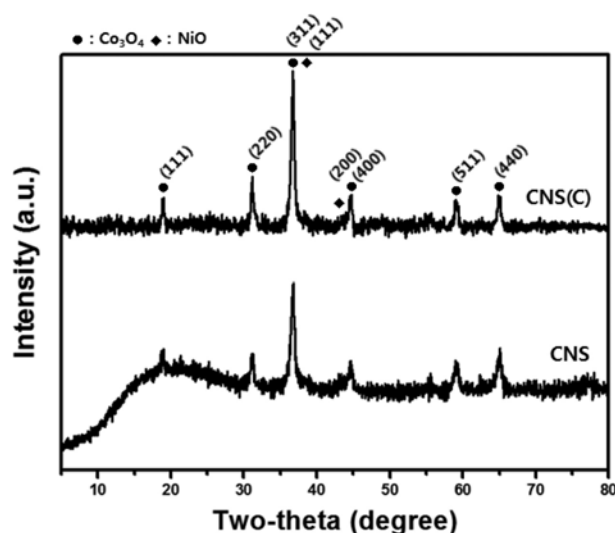Fig. 1. Pore size distribution of the fresh CNS catalysts.



Fig. 2. XRD patterns of the fresh CNS catalysts before FTS reaction.

pore size of ~7 nm assigned to the pores of SiO₂, at the pore size of ~4 nm assigned to the inter-structural pores formed between cobalt (or nickel) oxides and SiO₂, and at ~10 nm (mainly observed on the CNS(C)) assigned to the inter-structural pores between the deposited cokes and CNS possibly. This observation can be responsible for a larger surface area of 194 m²/g of the CNS(C) even after the coke deposition after the CDR reaction.

XRD patterns of the fresh CNS catalysts are displayed in Fig. 2 and the characteristic diffraction peaks of Co₃O₄ are clearly observed at $2\theta$=18.9, 31.2, 36.8, 44.7, 59.2 and 65.1° corresponding to the (111), (220), (311), (400), (511), and (440) planes, respectively [12]. In addition, the characteristic diffraction peaks of NiO were insignificantly observed at 37.1 and 43.1° due to the highly dispersed Ni species, which can be assigned to the (111) and (200) reflections of the NiO particles [13,14]. Due to the overlap of the characteristic diffraction peaks of Co₃O₄ and NiO at $2\theta$=~37°, the average particle size of Co₃O₄ was calculated by using the FWHM value of the diffraction peak at $2\theta$=44.7°. The calculated particle sizes of Co₃O₄ are 14.9 and 15.8 nm on the fresh CNS and used CNS(C), respectively, as summarized in Table 1. Furthermore, the calculated metallic cobalt particle size was found to be above 11 nm without significant size differences on the CNS catalysts, which has been also reported as the particle size showing little effects for changing the intrinsic FTS activity [11,12,15-17]. The surface area of metallic cobalt measured from H₂ chemisorption analysis was somewhat smaller on the CNS(C) with a value of 34.3 m²/$g_{Co}$ compared with that of 37.6 m²/$g_{Co}$ on the CNS due to the local formation of a larger Co₃O₄ particle without significant differences.

These similar physicochemical characters of the CNS and CNS(C) seem to show insignificant changes for the FTS activity; however, the advantages of the carbon-coating effects of the Ni/SiO₂ were significantly confirmed through the reduction behaviors of the deposited cobalt particles, especially on the CNS(C) as shown in Fig. 3 and Table 1. The fresh CNS showed three distinctive reduction peaks, with an additional peak at the highest reduction temperature above 600 °C, which can be attributed to the reduction of
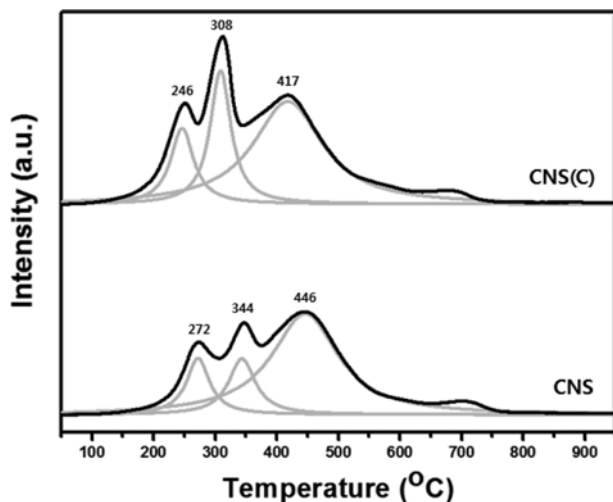
**Fig. 3. TPR profiles of the CNS catalysts.**

the strongly interacting NiO particles to metallic Ni on the $SiO_2$ support [10,13,14,18]. The reduction peak in the range of 200-400 °C can be attributed to the stepwise reduction of supported bulk $Co_3O_4$ to metallic cobalt through CoO intermediate formation ($Co_3O_4 \rightarrow CoO \rightarrow Co$), which are, respectively, assigned to the peaks of P(I) and P(II). The reduction of strongly interacting cobalt oxides to metallic cobalt or partial reduction of NiO was also observed at above 400 °C [19,20]. The first peak (assigned to P(I)) at the lower temperatures of 200-300 °C can be assigned to the reduction of the segregated $Co_3O_4$ particles, and the second sharp reduction peak (assigned to P(II)) at around 300-400 °C can be assigned to the

reduction of the larger bulk $Co_3O_4$ particles to the CoO species followed by full reduction of CoO to metallic cobalt above 400 °C, which seems to be strongly interacting with the $Ni/SiO_2$ or the deposited coke species [12,19,20]. Interestingly, all characteristic peaks shifted to lower temperature regions on the CNS(C) compared with the CNS, such as from 272 to 242 °C and 344 to 308 °C. These temperature shifts strongly suggest the suppressed metal-support interaction on the CNS(C) compared with the CNS. It is mainly attributed to the presence of the encapsulated carbons on the $Ni/SiO_2$ surfaces after CDR reaction by showing an insignificant effect for the cobalt particle size distribution during the catalyst preparation. In addition, the calculated degree of reduction from the values of P(I)+P(II)/total was, respectively, found to be around 0.298 and 0.400 on the CNS and CNS(C), which also suggests the facile reduction of cobalt particles on the CNS(C) by suppressing the metal-support interaction. In addition, as summarized in supplementary Table S1, the degree of reduction of the $Co_3O_4$ particles was further measured by $O_2$ titration, and the values were found to be around 50.3 and 57.7% on the CNS and CNS(C), respectively. This observation strongly suggests easy reduction behavior of the $Co_3O_4$ particles on the CNS(C) due to the mitigated cobalt-support interaction on the carbon-coated $Ni/SiO_2$ possibly.

The coke deposition and morphology on the used $Ni/SiO_2$ were further supported by SEM images as shown in Fig. 4. The deposited coke on the fresh $Ni/SiO_2$ (Fig. 4(a)) after CDR reaction in a fluidized-bed reactor was found to be mainly in the form of filamentous carbon by partially encapsulating the nickel particles as shown in Fig. 4(b). From the TEM analysis shown in Fig. 4(c) and Fig. 4(d), the cobalt particles on the CNS(C) were more homogeneously dispersed with particle sizes of 10-20 nm on the surfaces
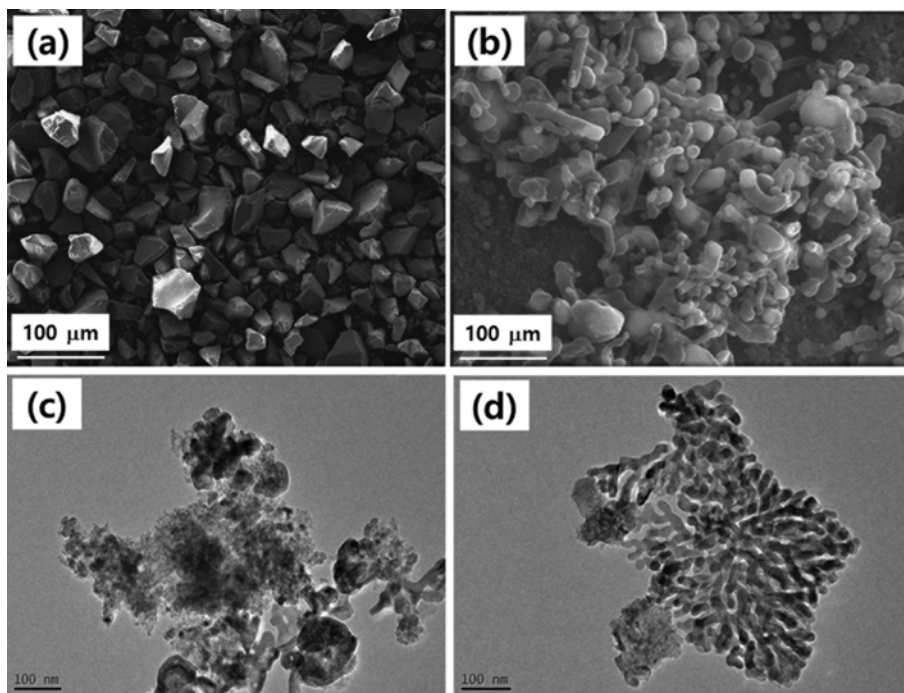


**Fig. 4. SEM images of the $Ni/SiO_2$; (a) before CDR reaction and (b) after CDR reaction at the molar feed molar ratio of $CH_4/CO_2=2$, and TEM images of the fresh CNS catalysts; (c) CNS and (d) CNS(C).**

**Table 2. Catalytic performances of the CNS catalysts**

| Catalysts | Activity[a] | | | Product distributions (C-mol%) | | | |
|---|---|---|---|---|---|---|---|
| | CO conv. (C-mol%) | Rate[b] (×10⁻⁶) | TOF (×10²)[c] | $C_1$ | $C_2$-$C_4$ | $C_5$+ | Olefins in $C_2$-$C_4$ |
| CNS | 8.6 | 1.35 | 0.6 | 14.7 | 11.2 | 74.1 | 41.1 |
| CNS(C) | 16.9 | 2.65 | 1.5 | 15.9 | 10.8 | 73.2 | 21.0 |

[a]FTS reaction was at the following reaction conditions; T=230 °C, P=2.0 MPa, WHSV=4000 L/(kg$_{cat}$·h), and feed gas composition of $H_2$/$N_2$/CO=62.84/5.60/31.56

[b]Reaction rate was defined as the reacted CO moles/($g_{cat}$·s)

[c]Turnover frequency (TOF) was defined as the reacted CO molecules/(surface cobalt atom·s)

of the carbon deposited Ni/SiO₂ surfaces compared with the CNS, where the cobalt particles on the CNS were significantly segregated on the outer Ni/SiO₂ surfaces as shown in Fig. 4(d). We believe that the good dispersion of cobalt particles with reduced metal-support interaction on the CNS(C) shown in Fig. 4(c) can be responsible for the enhanced FTS activity due to the enhanced reducibility and the suppressed metal-support interaction.

**2. Catalytic Activity of the CNS Catalysts**

The catalytic performance, such as CO conversion, reaction rate defined as the reacted CO mmoles/($g_{cat}$·s), and turnover frequency (TOF) defined as the reacted CO molecules/(surface cobalt atoms), and product distributions on the two CNS catalysts, is summarized in Table 2. CO conversion was found to be 8.6 and 16.9% on the CNS and CNS(C), respectively, with the similar product distributions such as $C_5$+ selectivity of ~74% and $CH_4$ selectivity of 15%. The reaction rate and TOF were found to be superior on the CNS(C) with the respective values of 2.65 mmoles/($g_{cat}$·s) and 0.015 molecules/(surface cobalt atoms) than those of the CNS with the values of 1.35 mmoles/($g_{cat}$·s) and 0.006 molecules/(surface cobalt atoms). Interestingly, olefin selectivity in the $C_2$-$C_4$ hydrocarbons was lower on the CNS(C) than the CNS possibly due to facile hydrogenation of the olefins formed on the reduced cobalt surfaces [12,15]. For the activity comparison with the CNS(C), mesoporous carbon support such as CMK-3 [21] was further tested for FTS reaction; the results are summarized in supplementary Table S1 and Fig. S3. The catalytic performance, such as CO conversion and reaction rate and product distribution on the CNS(C) and Co/CMK-3, was found to be similar, which suggests that the present carbon modified Ni/SiO₂ reforming catalysts with a proper preparation of the cobalt-based FTS catalyst can largely enhance the FTS activity without using a complicated fabrication method for the preparation of the regular mesoporous carbon support. Therefore, the carbon encapsulation of the Ni/SiO₂ during CDR reaction can modify the metal-support interaction by increasing the reducibility of cobalt particles as confirmed by TPR and $O_2$ titration. The enhanced catalytic activity on the CNS(C) for the FTS reaction seems to be mainly attributed to the modification of the Ni/SiO₂ surfaces by forming encapsulated carbons. As shown in Fig. 5, the catalytic activity on the CNS(C) steadily increased up to 10 h on stream, and it stabilized due to the possible surface activation steps of metallic cobalt particles [22]. This continuous activity increase on the CNS(C) from the very beginning of reaction compared with that of the CNS, which showed a stable and lower activity at the very beginning of reaction, can be possibly attributed to the lessened metal-support
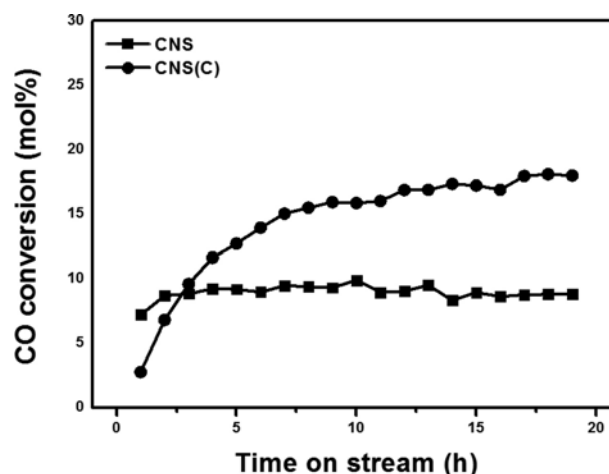


**Fig. 5. Catalytic activity of the CNS catalysts with time on stream (h).**

interactions by reconstructing the metallic cobalt surfaces such as the possible redispersion or segregation of the supported cobalt particles [1,19,22] on the carbon deposited Ni/SiO₂ surfaces. The cobalt particle sizes on the CNS and CNS(C) after the FTS reaction were also measured by XRD as shown in Fig. S4. The intense characteristic diffraction peak of (400) plane of the $Co_3O_4$ at $2\theta=$ 44.7° was clearly observed on the used CNS catalysts after 20 h on stream, and the particle sizes were found to be somewhat larger on the CNS(C) with 25.4 nm compared to that of 24.0 nm on the used CNS without significant variations. Based on the above observation, we believe that the observed higher catalytic activity on the CNS(C) can be attributed to the homogeneous distribution of cobalt particles compared with the CNS and the modified metal-support interaction on the carbon deposited Ni/SiO₂ surfaces by increasing the reducibility of cobalt oxides. The characteristics of the carbon-coated CNS(C) catalyst can be the fundamental preparation method to modify the metal-support interaction during the cobalt-based FTS catalyst preparation through the easy modification using carbon sources of the commercially available supports.

**CONCLUSIONS**

The carbon-coated Ni/SiO₂ after CDR reaction can be successfully applied for the cobalt-based FTS catalyst preparation by showing superior activity due to the mitigated metal-support interaction.

The deposited carbons on the $Ni/SiO_2$ after CDR reaction were mainly in the types of the filamentous or encapsulated carbons, and it significantly enhanced CO conversion and intrinsic catalytic activity of TOF without significant changes of the hydrocarbon distributions on the CNS(C) catalyst. The deposited carbons on the $Ni/SiO_2$ play an important role in increasing the reducibility and the homogeneous size distribution of the active cobalt particles through the mitigated metal-support interaction. The enhancement of the FTS activity on the cobalt-based catalysts can be obtained through a proper carbon modification of the $Ni/SiO_2$ surfaces through the encapsulation of nickel surfaces.

## ACKNOWLEDGEMENTS

## SUPPORTING INFORMATION

Additional information as noted in the text. This information is available via the Internet at http://www.springer.com/chemistry/journal/11814.

## REFERENCES

1. A. Y. Khodakov, W. Chu and P. Fongarland, *Chem. Rev.*, **107**, 1692 (2007).
2. T. Fu, R. Liu, J. Lv and Z. Li, *Fuel. Process. Technol.*, **122**, 49 (2014).
3. H. Xiong, M. A. M. Motchelaho, M. Moyo, L. L. Jewell and N. J. Coville, *J. Catal.*, **278**, 26 (2011).
4. T. Fu, Y. Jiang, J. Lv and Z. Li, *Fuel. Process. Technol.*, **110**, 141 (2013).
5. S. H. Kang, K. J. Woo, J. W. Bae, K. W. Jun and Y. Kang, *Korean J. Chem. Eng.*, **26**(6), 1533 (2009).
6. M. Zaman, A. Khodadi and Y. Mortazavi, *Fuel. Process. Technol.*, **90**, 1214 (2009).
7. A. M. Saib, M. Claeys and E. van Steen, *Catal. Today*, **71**, 395 (2002).
8. K. Pinkaew, P. Praserthdam and B. Jongsomji, *Korean J. Chem. Eng.*, **30**(1), 50 (2013).
9. S. He, H. Wu, W. Yu, L. Mo, H. Lou and X. Zheng, *Int. J. Hydrogen Energy*, **34**, 839 (2009).
10. Y. K. Han, C. I. Ahn, J. W. Bae, AR. Kim and G. Y. Han, *Ind. Eng. Chem. Res.*, **52**, 13288 (2013).
11. D. Schanke, S. Vada, E. A. Blekkan, A. M. Hilmen, A. Hoff and A. Holmen, *J. Catal.*, **156**, 85 (1995).
12. H. M. Koo, B. S. Lee, M. J. Park, D. J. Moon, H. S. Roh and J. W. Bae, *Catal. Sci. Technol.*, **4**, 343 (2014).
13. L. Yao, J. Zhu, X. Peng, D. Tong and C. Hu, *Int. J. Hydrogen Energy*, **38**, 7268 (2013).
14. H. P. Ren, Y. H. Song, Q. Q. Hao, Z. W. Liu, W. Wang, J. G. Chen, J. Jiang, Z. T. Liu, Z. Hao and J. Lu, *Ind. Eng. Chem. Res.*, **53**, 19077 (2014).
15. B. S. Lee, I. H. Jang, J. W. Bae, S. H. Um, P. J. Yoo, M. J. Park, Y. C. Lee and K. W. Jun, *Catal. Surv. Asia*, **16**, 121 (2012).
16. A. Y. Khodakov, A. Griboval-Constant, R. Bechara and F. Villain, *J. Phys. Chem. B*, **105**, 9805 (2001).
17. B. Zeng, B. Hou, L. Jia, J. Wang, C. Chen, Y. Sun and D. Li, *ChemCatChem*, **5**, 3794 (2013).
18. S. D. Robertson, B. D. McNicol, J. H. de Bass and S. C. Kloet, *J. Catal.*, **37**, 424 (1975).
19. T. Koh, H. M. Koo, T. Yu, B. Lim and J. W. Bae, *ACS Catal.*, **4**, 1054 (2014).
20. M. H. Woo, J. M. Cho, K. W. Jun, Y. J. Lee and J. W. Bae, *ChemCatChem*, **7**, 1460 (2015).
21. D. P. Upare, S. Yoon and C. W. Lee, *Korean J. Chem. Eng.*, **28**(3), 731 (2011).
22. E. Iglesia, *Appl. Catal. A*, **161**, 59 (1997).